International Core Journal of Engineering Volume 7 Issue 2, 2021
ISSN: 2414-1895 DOI: 10.6919/ICJE.202102_7(2).0036

The Design of High-frequency Vibratory Stress Relief Device

Zhipeng Huo[1,a], Bangping Gu[1,b], Zidi Jin[2,c], Zhongshan Wang[1,d], Ping Wang[1,e], Xiong Hu[1,f], Guanhua Xu[3,g] and Jintao Lai[4,h]

[1]Logistics Engineering College, Shanghai Maritime University, Shanghai 201306, China;

[2]Beijing Geolight Technology Co., Ltd., Beijing 102628, China;

[3]Zhejiang University, Hangzhou 310027, China;

[4]Shaoxing University, Shaoxing 312000, China.

[a]zp_huo2020@163.com, [b]11025033@zju.edu.cn, [c]jinzidi55@163.com, [d]zswang_white@163.com, [e]18201750773@163.com, [f]huxiong@shmtu.edu.cn, [g]xgh_zju@163.com, [h]usxljt88@163.com

Abstract

In order to improve the effect of high-frequency vibratory stress relief (VSR) on the small work-piece, a high-frequency VSR device was designed. The ANSYS was employed to carry out numerical modal analysis of the small work-piece. Then a high-frequency vibration energy amplification device and a clamping device were designed. Strain gauges were attached at the distribution region of the peak residual stress. The small work-piece was clamped by the clamping device. In this case, the small work-piece can be vibrated according to its mode shape. The effect of the high-frequency VSR can be improved by the high-frequency VSR device designed in this paper.

Keywords

High-Frequency VSR; Vibration Energy Amplification Device; Clamping Device.

1. Introduction

Vibratory stress relief (VSR) technology has the advantages of good processing effect, low energy consumption, short processing time, energy saving and less environmental pollution [1-4]. In this case, the VSR technology has been widely used in the mechanical engineering field. A speed-adjustable motor is adopted as the exciter for the traditional low-frequency VSR technology [5], which results in that the excitation frequency of the traditional low-frequency VSR is generally less than 200 Hz. Under this condition, the optional vibration modes for the traditional low-frequency VSR are very limited. The electromagnetic exciter is adopted as the exciter for the high-frequency VSR technology [6-7]. In this case, the vibration frequency of the electromagnetic exciter can reach 10 kHz, which implies that the application range of the VSR technology can be extended. However, the output vibration energy of the electromagnetic exciter is very limited, which results in that the effect of the high-frequency VSR is very poor when the small work-piece is directly clamped on the electromagnetic exciter. In the current high frequency VSR technology [6-9], the acceleration vibration level is used to represent the vibration energy, which results in that it is incapable to evaluate whether the residual stress on the small work-piece can be eliminated or not. Meanwhile, the sweeping frequency method is used to determine the excitation frequency for the high-frequency VSR technology. This frequency determination method has the following shortcomings. Firstly, it takes some time and reduces the efficiency. Secondly, the distribution of the residual stress on the small work-piece is not considered when the excitation frequency of the high-frequency VSR is determined

ISSN: 2414-1895 DOI: 10.6919/ICJE.202102_7(2).0036

by the sweeping frequency method. In addition, the small work-piece is rigidly mounted on the supporting platform, which results in that it is difficult for the small work-piece to vibrate according to its mode shape. So the effect of the high-frequency VSR on the small work-piece is limited. In order to solve the above problems, a high-frequency VSR device was designed in this study to improve the effect of the high-frequency VSR.

2. Design of High-frequency VSR Device

The high-frequency VSR device is shown in Figure 1, which comprises a high-frequency vibration energy amplification device, a clamping device, cushion blocks, strain gauges, a dynamic strain meter, a host computer system, a signal generator, a power driver and an electromagnetic exciter.

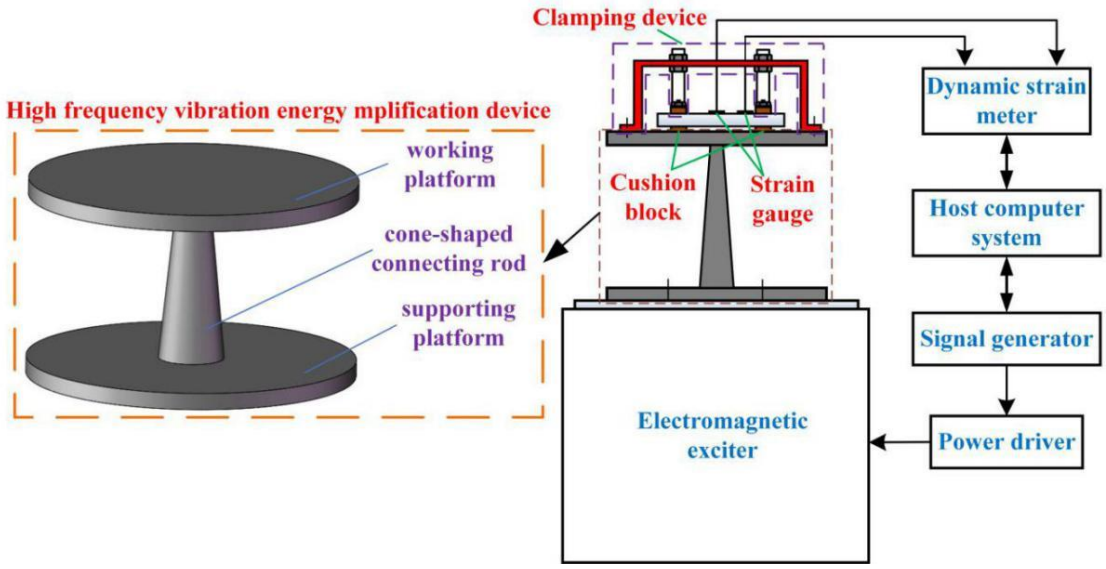

Figure 1. High-frequency VSR device

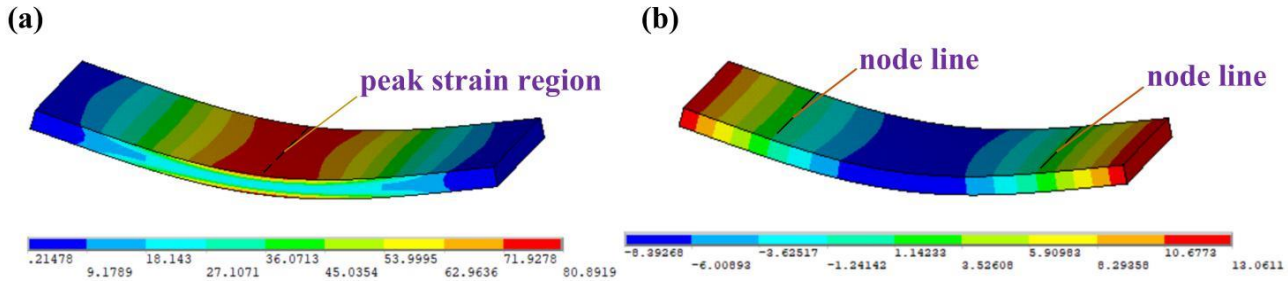

Figure 2. (a) The first-order bending strain mode of the small work-piece
(b) The first-order bending displacement mode of the small work-piece

2.1 Numerical Modal Analysis

The small work-piece is a 45# steel plate small work-piece and its size is $60 \times 20 \times 2.5$ mm. The density ρ is 7850 kg/m^3, elastic modulus E is 200 GPa and Poisson's ratio ν is 0.28. The ANSYS was used for numerical modal analysis. The first-order bending strain mode and the peak strain region on the small work-piece are shown in Figure 2(a). The first-order bending displacement mode and the node lines of the small work-piece are shown in Figure 2(b). The laser surface processing was used to generate the initial residual stress on the small work-piece. When the peak strain region on the small work-piece is consistent with the peak residual stress region on the small work-piece, the bending vibration frequency of a certain order corresponding to the bending strain mode of a certain

ISSN: 2414-1895 DOI: 10.6919/ICJE.202102_7(2).0036

order is recorded as the target frequency. In order to simplify the analysis, the peak residual stress region on the small work-piece is consistent with the peak strain region of the first-order bending strain mode. So the first-order bending vibration frequency was recorded as the target frequency *f*, whose value is 3592.4 Hz.

2.2 The High-frequency Vibration Energy Amplification Device

The high-frequency vibration energy amplification device is shown in Figure 1. Compared with the high-frequency vibration energy amplification device shown in the references [8-9], the cone-shaped connecting rod adopted in this paper has a lighter weight if the diameter of the large end of the cone-shaped connecting rod is same as the diameter of the cylindrical connecting rod. In this case, it is beneficial for the excitation of the high-frequency VSR device. The orthogonal experimental design method is used to optimize the design of the high frequency vibration energy amplification device. In this study, the natural frequency f_a of the first-order axial vibration of the high-frequency vibration energy amplification device was regarded as the target of the optimization design, and the structural dimensions were regarded as the variables. The scheme corresponding to a minimum value of the deviation between f_a and f was selected as the structural dimensions scheme. The optimization design steps based on orthogonal experimental design method are as follows:

The length *l* of the cone-shaped connecting rod, the diameter *d* of the small end of the cone-shaped connecting rod and the thickness *h* of the working platform were selected as the factors, and three levels were selected for each factor. In order to improve the efficiency of optimization design, the other structural dimensions were set as the fixed values. In this study, the diameter of the working platform and the diameter of the supporting platform are 100 mm, the thickness of the supporting platform is 8 mm, and the diameter of the large diameter of the cone-shaped connecting rod is 11 mm; $L_9(3^4)$ orthogonal experimental table was selected to make the schemes of the optimization design. The material of the high-frequency vibration energy amplification device is aluminum alloy. The natural frequency f_a of the first order axial vibration of each scheme was obtained by ANSYS. The deviation between f_a and f is defined as $\frac{|f-f_a|}{f}\times 100\%$. The deviation of each scheme is calculated and the results are listed in Table 1.

Table 1. The schemes based on the orthogonal experiment table $L_9(3^4)$ and results

Schemes	Structural dimensions			Results	
	l(mm)	d(mm)	h(mm)	f_a (Hz)	$\frac{\lvert f-f_a\rvert}{f}\times 100\%$
1	40	8	9	3449.2	3.98%
2	40	9	10	3611.5	0.53%
3	40	10	11	3717.1	3.47%
4	50	8	10	3522.8	1.94%
5	50	9	11	3636.1	1.22%
6	50	10	9	3538.9	1.49%
7	60	8	11	3549.3	1.20%
8	60	9	9	3451.5	3.92%
9	60	10	10	3599.4	0.19%

Based on the results shown in Table 1, the deviation between f_a and *f* is the smallest for the scheme 9. In this case, the effect of high-frequency VSR can be improved. Thus, the scheme 9 is selected as the structural dimensions scheme of the high-frequency energy amplification device.

ISSN: 2414-1895 DOI: 10.6919/ICJE.202102_7(2).0036

2.3 The Clamping Device

The clamping device is shown in Figure 3, which comprises an adjusting device and pressing devices.

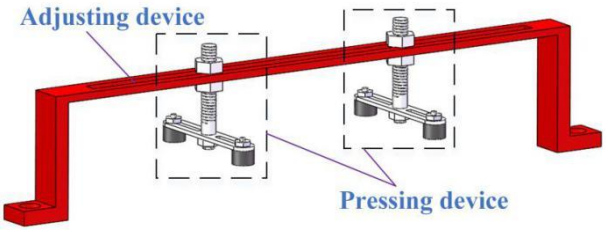

Figure 3. The clamping device

2.4 Attaching the Strain Gauges

The strain gauges were attached on the peak residual stress of the small work-piece, where the first strain gauge was attached along the first principal stress direction and the second strain gauge was attached along the second principal stress direction.

3. Application of High-frequency VSR Device

3.1 Clamping the Small Work-piece

As shown in Figure 4, the small work-piece was clamped on the working platform at the vibration node lines of the small work-piece by the clamping device, and the cushion blocks were set along the vibration node lines on the small work-piece.

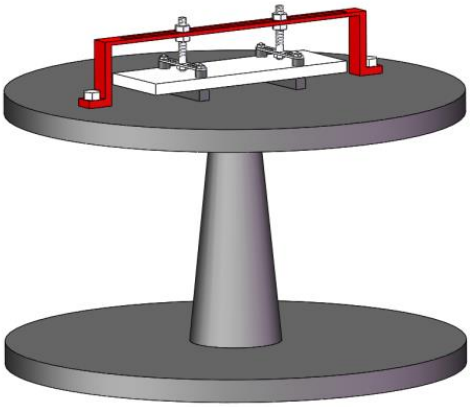

Figure 4. Clamping the small work-piece

3.2 High-frequency VSR Process

The host computer system controls the signal generator to output the excitation frequency *f* of the high-frequency VSR. Then the high-frequency vibration can be generated by the electromagnetic exciter, and the high-frequency VSR on the small work-piece was carried out based on the high-frequency VSR device as shown in Figure 1. The strain signal on the small work-piece was collected by the dynamic strain meter. The peak strain obtained by the first strain gauge is ε_1, and the corresponding dynamic stress acting on the direction of the first principal stress σ_{r1} is

$$\sigma_1 = E\varepsilon_1 \tag{1}$$

The peak strain obtained by the second strain gauge is ε_2, and the corresponding dynamic stress acting on the direction of the second principal stress σ_{r2} is

ISSN: 2414-1895 DOI: 10.6919/ICJE.202102_7(2).0036

$$\sigma_2 = E\varepsilon_2 \tag{2}$$

The output current of the power driver can be adjusted during the high-frequency VSR process. Under this condition, the high-frequency vibration energy output by the electromagnetic exciter can be adjusted. That is, the dynamic stress acting on the small work-piece can be changed during the high-frequency VSR process. When the sum of σ_1 and σ_{r1} and the sum of σ_2 and σ_{r2} meet the relationship $\sigma_s < \sigma_1 + \sigma_{r1} < \sigma_p$ and $\sigma_s < \sigma_2 + \sigma_{r2} < \sigma_p$, the first principal stress σ_{r1} and the the second principal stress σ_{r2} can be eliminated by the high-frequency VSR.

4. Conclusion

1. The output vibration energy of the electromagnetic exciter can be amplified by the high-frequency vibration energy amplification device when the high-frequency VSR on the small work-piece is carried out under the natural frequency of the first-order axial vibration of the high-frequency vibration energy amplification device. In this case, the high-frequency vibration energy acting on the small work-piece is improved.

2. The excitation frequency of the high-frequency VSR can be determined according to the method of the numerical modal analysis, which improves the efficiency of the high-frequency VSR.

3. The small work-piece can vibrate according to its mode shape based on the high-frequency VSR device designed in this paper. In this case, the effect of the high-frequency VSR can be improved.

Acknowledgments

This research is sponsored by the National Natural Science Foundation of China for Young Scholars (Nos. 51605303 and 51805477).

References

[1] H.J. Gao, Y.D. Zhang, Q. Wu, et al. Fatigue life of 7075-T651 aluminium alloy treated with vibratory stress relief. Intenational journal of fatigue, Vol. 108 (2018), p.62-67.

[2] M.J. Vardanjani, M. Ghayour, R.M. Homami. Analysis of the Vibrational Stress Relief for Reducing the Residual Stresses Caused by Machining. Experimental Techniques, Vol. 40 (2016), No. 2, p.705-713.

[3] J.S. Wang, C.C. Hsieh, C.M. Lin, et al. The effect of residual stress relaxation by the vibratory stress relief technique on the textures of grains in AA 6061 aluminum alloy. Materials science & engineering A, Vol. 605 (2014), p.98-107.

[4] S.M. Ebrahimi, M. Farahani, D. Akbari. The influences of the cyclic force magnitude and frequency on the effectiveness of the vibratory stress relief process on a butt welded connection. The International Journal of Advanced Manufacturing Technology, Vol. 102 (2019), No. 5-8, p.2147-2158.

[5] M. Hu, C.W. Yu, J. Zhang, et al. Accuracy Stability for Large Machine Tool Body. Journal of Xi'an Jiaotong University, Vol. 48 (2014), No. 6, p.65-73. (In Chinese).

[6] J.W. Wang, W. He. Research on the Technology of High Frequency Vibratory Stress Relief. Machine tool & hydraulics, (2005), No. 9, p.9-11, 94. (In Chinese).

[7] G. Jiang, W. He, J.Y. Zheng. Mechanism and experimental research on high frequency vibratory stress relief. Journal of Zhejiang University (Engineering Science), Vol. 43 (2009), No. 7, p.1269-1272. (In Chinese).

[8] B.P. Gu, X. Hu, J.T. Lai, et al. Effects of high-frequency vibration on quenched residual stress in Cr12MoV steel. Journal of Materials Research, Vol. 31 (2016), No. 22, p.3588-3596.

[9] B.P. Gu, D.J. Kong, J.T. Lai, et al. Optimization design and experimental study of a high-frequency vibration energy amplification device. Journal of Vibration and shock, Vol. 36 (2017), No. 12, p.243-248. (In Chinese).